

# Estimating Individual Layer Properties from Well Testing Data in Stratified Reservoirs with Multilateral Wells

Renan Vieira Bela · Sinésio Pesco · Abelardo  
Borges Barreto Jr. · Mustafa Onur

the date of receipt and acceptance should be inserted later

**Abstract** One of the main purposes for conducting well tests is to obtain information about reservoir parameters, such as its permeability and the existence of skin effects. Determining individual layer properties from pressure transient data in multilayer reservoirs is challenging, since pressure behavior is influenced by the properties of all layers. This work extends two existing methods for estimating individual layer properties in multilayer systems with vertical wells to stratified reservoirs with multilateral horizontal wells. These methods are the rate-normalized pressure analysis and the delta transient method. Both methods require a clear identification of radial flow regimes, which may not occur in a practical case. We show that the Nelder-Mead global method algorithm can also be used to evaluate layer permeabilities and skin. This method represents an alternative to estimate layer parameters in cases where radial flow regimes are difficult to identify or nonexistent, since it does not depend on the occurrence of any specific flow regime. The proposed techniques are applied on a pair of synthetic cases, where pressure and layer flow-rate profiles are computed from a previously existing analytical model. Results show that all three methods are able to yield good estimates for layer horizontal and vertical permeabilities, but only the Nelder-Mead method is able to accurately estimate the individual skin factors. Moreover, the Nelder-Mead method can provide good estimates for layer properties even if late-time radial flow is not observed. Nonetheless, our results suggest that early-time data is critical to estimate layer vertical permeabilities and mechanical skin.

**Keywords** Well Testing · Multilateral Wells · Stratified Reservoirs · Rate-normalized pressure analysis · Delta transient method · Nelder-Mead algorithm

## 1 Introduction

Reservoir characterization is a major goal of well testing. Based on the pressure response measured during the test, it is possible to estimate reservoir features such as permeability, average pressure, skin factor and outer boundary condition. In multilayer systems, it is desirable to obtain information regarding each individual layer, so that the reservoir productivity may be more accurately estimated.

In multilayer stratified systems, conventional interpretation techniques allow the determination of the reservoir equivalent permeability and skin (Cobb et al., 1972; Raghavan et al., 1974; Larsen, 1982; Kuchuk et al., 1986a; Ehlig-Economides and Joseph, 1987; Raghavan, 1989; Kuchuk and Wilkinson, 1991). Computing individual layer properties, however, is not so straightforward, since

---

R. V. Bela (✉) · S. Pesco · A. B. Barreto Jr.  
Departamento de Matemática - PUC-Rio  
E-mail: renanvb1@mat.puc-rio.br

M. Onur  
McDoughall School of Petroleum Engineering - The University of Tulsa

pressure response at the wellbore is simultaneously influenced by all layers (Lefkovits et al., 1961; Cobb et al., 1972; Kuchuk et al., 1986b; Guimarães and Galvão, 2017).

Larsen (1982) applied the analytical approximation proposed by Larsen (1981) for pressure behavior in two-layered commingled reservoirs with vertical wells to obtain estimates for layer flow capacities and skin. Layer properties are determined through a trial-and-error procedure that aims to match the observed pressure data and the theoretical pressure response obtained using the analytical expression developed by Larsen (1981). If data are sufficiently smooth, then layer properties may be evaluated using analytical expressions, instead of a trial-and-error procedure. Larsen (1982) also stated that this procedure could be applied in reservoirs with crossflow, provided that data after crossflow effects become relevant are avoided.

A method to evaluate layer properties in reservoirs with unequal initial pressure was derived by Aly et al. (1994). Their method, which is called Derivative Extreme Method, is based on the pre-production pressure data, rather than conventional well testing. It consists of identifying the point where pressure derivative attains its extreme (maximum or minimum) value. Then, a system of equations is built so that layer properties such as permeabilities, skin factors and porosities may be computed.

Gao (1987) proposed a means to determine layer permeabilities in a two-layer reservoir with vertical wellbore from well testing data. The method consists of isolating the layers with packers so that individual well test analysis may be performed for each layer. Thereby, conventional single-layer interpretation methods may be applied to obtain layer permeabilities and skin factors.

As pointed out by Raghavan (1989), isolating the layers and running individual pressure transient tests for each one of them is often unfeasible in practice. Therefore, Raghavan (1989) claimed that the rate-normalized pressure analysis (or RNPA) represents a more viable alternative to determine individual layer properties. This technique was first introduced by Ehlig-Economides and Joseph (1987), in a work that also provided a detailed description of the analytical model for single-phase flow in multilayer reservoirs with vertical wells. RNPA, however, presents an intrinsic operational setback, as it requires several measurements of layer flow-rates.

An alternative solution was developed by Guimarães and Galvão (2017). In their work, a new layer parameter denoted as "delta transient" is defined. Based on production logging data from merely two distinct time steps, the delta transient parameter is determined and, hence, so are layer permeabilities and skin factors. Their work presents a strong operational drive by requiring only a few hours of rig time to acquire the test data. In a further work, Galvão and Guimarães (2017) extended the delta transient method (or DTM) to tests with a multiple flow-rates scheme.

All the methods mentioned above present one common feature: they were designed for multilayer reservoirs with vertical wells. Thereby, current approaches to estimate individual layer parameters are not suitable for reservoirs with horizontal wells. Interest in drilling horizontal wells has been increasing, as they present some benefits compared to vertical wells. They mitigate fluid coning effects and their performance is superior in reservoirs with high vertical permeability (Clonts and Ramey Jr., 1986; Ozkan et al., 1989; Algharaib et al., 2006). Moreover, one horizontal well may produce the same amount of oil as several vertical wells (Joshi, 2003). Horizontal wells also present high productivity, due to their larger contact area with the reservoir (Algharaib et al., 2006; Biryukov and Kuchuk, 2015). However, to the best of our knowledge, there is currently no reliable interpretation technique to obtain estimates for individual layer properties from pressure data collected during well testing in stratified reservoirs with multilateral horizontal wells.

Thus, the main purpose of this work is to achieve a means of determining individual layer permeabilities and skin factors from well testing data in multilayer reservoirs with horizontal wellbores. In this paper, the RNPA (Ehlig-Economides and Joseph, 1987; Raghavan, 1989) and the DTM (Galvão and Guimarães, 2017; Guimarães and Galvão, 2017) are extended so that they can be applied in horizontal wells also. Both RNPA and DTM demand nothing more than a general worksheet software to be performed.

The proposed extensions of RNPA and DTM rely on the identification of the two distinct radial flow regimes that might occur during single-phase flow in horizontal wells: one at early times, while the vertical boundaries are not felt by the wellbore and another at late times, when pressure diffusion

propagates radially in the horizontal plane (Rosa and Carvalho, 1989; Jelmert and Thompson, 1991; Kuchuk, 1995; Nie et al., 2011).

Yet, depending on the reservoir properties and test duration, sometimes no radial flow regime may be observed. In those cases, optimization methods consist of an alternative to pressure transient interpretation techniques. Reservoir parameters are estimated by minimizing an objective function, so that the computed parameters yield pressure and flow-rate responses that match the observed data. In this context, gradient-free methods are usually desired, since they are more computationally efficient. The Nelder-Mead method (also referred to as simplex or polytope method) is a global optimization algorithm that aims to find a set of parameters that minimize the objective function by sequentially applying four simple operations: reflection, expansion, contraction and shrinkage (Nelder and Mead, 1965; Barati, 2011; Feng et al., 2020). It may be used to estimate reservoir parameters by matching pressure data (Rahmati et al., 2013) when coupled with analytical models.

There exist analytical solutions for pressure behavior in single-layer reservoirs with horizontal wells both in Laplace domain (Goode and Thambynayagam, 1987; Kuchuk et al., 1991) and in real space (Daviau et al., 1988; Ozkan et al., 1989). Analytical models for multilateral wells in multilayer reservoirs with multilateral horizontal wells are also available (Vo and Madden, 1995; Larsen, 2000; Yildiz, 2003; Pan et al., 2010). Layer flow-rate profiles may also be determined from those models. Thus, a third approach was conducted by using the analytical solution from Pan et al. (2010) as forward model for the Nelder-Mead global optimization algorithm (Nelder and Mead, 1965).

The paper is organized as follows: Section 2 presents the early- and late-time logarithmic approximations for pressure change, whereas Section 3 depicts the proposed techniques to determine layer permeabilities. The obtained results are displayed in Section 4. Finally, Section 5 presents the main conclusions of this work.

## 2 Logarithmic approximations for pressure change

The real space solution for single-phase flow of a slightly compressible fluid with constant compressibility and viscosity in reservoirs with multilateral horizontal wells was developed by Pan et al. (2010). Their model is outlined in Appendix A. Figure 1 displays a schematic of the reservoir model considered in this study. Eq. (A-1) and the linear system of equations given by Eq. (A-4) (given in Appendix A) apply at all times. Nonetheless, early- and late-time approximations can be derived, considering the distinct flow regimes observed in horizontal wells. Here and throughout, all equations are expressed in terms of consistent unit systems.

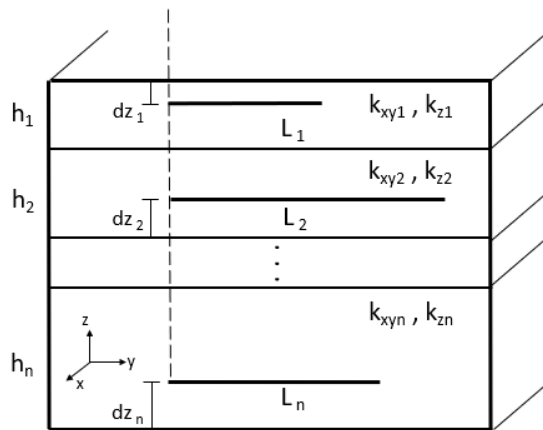


Fig. 1: Schematic of the Reservoir Model Considered in This Study

As evidenced in Fig. 1, layer properties such as permeability and thickness may be different in each layer. The considered model also accounts for distinct wellbore lengths and well off-centering. Therefore, the smallest distance between the wellbore and a vertical boundary (denoted as  $dz_j$ ) may be measured from the wellbore to the layer top boundary or to the layer bottom boundary, depending on the wellbore position.

## 2.1 Early-time approximation

Immediately after the wellbore is open, equipotential curves are concentric ellipses in the vertical plane perpendicular to the wellbore. A radial flow is observed, and pressure response is similar to a vertical well in an infinite acting reservoir whose thickness equals the horizontal wellbore length (Daviau et al., 1988; Rosa and Carvalho, 1989; Nie et al., 2011). While early-time radial flow occurs, an approximation for pressure change at the wellbore in a multilayer reservoir with a multilateral horizontal well is given by:

$$\Delta p_{wf}(t) = \frac{qB\mu}{L_t(k_{zx})_{eq}} \left[ \frac{1}{2} \ln \left( \frac{4(k_{zx})_{eq}t}{\exp(\gamma)\mu(\phi c_t)_{eq}r_w^2} \right) + S_{eq} \right], \quad (1)$$

where  $q$  stands for the production flow-rate,  $B$  stands for formation volume factor,  $\mu$  stands for oil viscosity,  $L_t$  stands for the wellbore total length and  $r_w$  stands for the wellbore radius. The equivalent permeability in the vertical plane, denoted as  $(k_{zx})_{eq}$ , is defined as:

$$(k_{zx})_{eq} = \frac{\sum_{j=1}^n L_j k_{zxj}}{L_t}, \quad (2)$$

where  $k_{zxj} = \sqrt{k_{xyj}k_{zj}}$  is the geometric mean permeability in the  $zx$ -plane for layer  $j$ . Besides, in Eq. (1),  $(\phi c_t)_{eq}$  represents a thickness weighted average of the porosity-compressibility product:

$$(\phi c_t)_{eq} = \frac{\sum_{j=1}^n \phi_j c_{tj} h_j}{h_t}. \quad (3)$$

In Eq. (1),  $S_{eq}$  denotes the equivalent mechanical skin factor. Analogously to the definition proposed by Ehlig-Economides and Joseph (1987), it may be computed as a weighted average of the skin factors in each layer:

$$S_{eq} = \frac{\sum_{j=1}^n k_{zxj} L_j S_j}{(k_{zx})_{eq} L_t}. \quad (4)$$

Eq. (1) is valid as long as the early-time radial flow is simultaneously occurring in all layers. Pressure change during early-time radial flow increases linearly with the natural logarithm of time. Thus, the equivalent permeability in the vertical plane  $(k_{zx})_{eq}$  can be estimated by taking the pressure derivative with respect to the natural logarithm of time (hereafter denoted simply as pressure derivative) (Yildiz, 2003):

$$\frac{\partial \Delta p_{wf}}{\partial \ln(t)} = m_{erf} = \frac{qB\mu}{2L_t(k_{zx})_{eq}} \longrightarrow (k_{zx})_{eq} = \frac{qB\mu}{2m_{erf}L_t}. \quad (5)$$

Thereby, after  $(k_{zx})_{eq}$  has been determined from Eq. (5), the equivalent mechanical skin may be computed as:

$$S_{eq} = \frac{1}{2} \left[ \frac{\Delta p_{wf}(t_{erf})}{m_{erf}} - \ln(t_{erf}) - \ln \left( \frac{4(k_{zx})_{eq}}{\exp(\gamma)\mu(\phi c_t)_{eq}r_w^2} \right) \right], \quad (6)$$

where  $t_{erf}$  is any chosen time during the early-time radial flow and  $\Delta p_{wf}(t_{erf})$  is its corresponding pressure change.

## 2.2 Late-time approximation

At late times, a pseudo-radial (or late-time radial) flow develops, as flow in the vertical direction becomes negligible and pressure diffusion propagates predominantly in the horizontal plane (Rosa and Carvalho, 1989; Odeh and Babu, 1990; Kuchuk et al., 1991; Nie et al., 2011). Once the late-time radial flow prevails in all layers, pressure response at the wellbore may be approximated by:

$$\Delta p_{wf}(t) = \frac{qB\mu}{h_t(k_{xy})_{eq}} \left[ \frac{1}{2} \ln \left( \frac{4(k_{xy})_{eq}t}{\exp(\gamma)\mu(\phi C_t)_{eq}r_w^2} \right) + S_{teq} \right], \quad (7)$$

where  $h_t$  stands for the reservoir total thickness. The equivalent permeability in the horizontal plane  $(k_{xy})_{eq}$  is defined as:

$$(k_{xy})_{eq} = \frac{\sum_{j=1}^n h_j k_{xyj}}{h_t}. \quad (8)$$

At late times, besides the mechanical damage, there is also a pseudo-skin effect due to the convergence of stream lines beyond the well tips (Goode and Thambynayagam, 1987; Kuchuk et al., 1991). Therefore, in Eq. (7),  $S_{teq}$  stands for the equivalent total skin factor. Analogously to Eq. (4), it consists of a weighted average of total skin factors in all layers:

$$S_{teq} = \frac{\sum_{j=1}^n k_{xyj} h_j S_{tj}}{(k_{xy})_{eq} h_t}. \quad (9)$$

where  $S_{tj}$  stands for the total skin factor in layer  $j$  and is defined as (Daviau et al., 1988):

$$S_{tj} = S_{gj} + \frac{k_{xyj} h_j}{k_{zxxj} L_j} S_j, \quad (10)$$

where  $S_{gj}$  stands for the pseudo-skin in layer  $j$ . For a laterally infinite reservoir, it is computed as (Daviau et al., 1988):

$$S_{gj} = \ln \left( \frac{4r_w}{L_j \left( \frac{2\pi r_w}{h_j} \right)^{e_j}} \right); \quad e_j = \frac{k_{xyj} h_j}{k_{zxxj} L_j}. \quad (11)$$

Eq. (7) shows that pressure change is a linear function of the natural logarithm of time. Therefore, pressure derivative during late-time radial flow may be used to evaluate the equivalent permeability in the  $xy$ -plane (Yildiz, 2003):

$$\frac{\partial \Delta p_{wf}}{\partial \ln(t)} = m_{lrf} = \frac{qB\mu}{2h_t(k_{xy})_{eq}} \rightarrow (k_{xy})_{eq} = \frac{qB\mu}{2m_{lrf} h_t}. \quad (12)$$

After the horizontal permeability has been computed, the equivalent total skin factor may be determined as:

$$S_{teq} = \frac{1}{2} \left[ \frac{\Delta p_{wf}(t_{lrf})}{m_{lrf}} - \ln(t_{lrf}) - \ln \left( \frac{4(k_{xy})_{eq}}{\exp(\gamma)\mu(\phi C_t)_{eq}r_w^2} \right) \right]. \quad (13)$$

where  $t_{lrf}$  is an arbitrary time during the late-time radial flow and  $\Delta p_{wf}(t_{lrf})$  is its corresponding pressure change.

The equivalent total skin factor defined in Eq. (9) represents a weighted average of the total skin factors in all layers, encompassing both stream lines geometry and mechanical damage around the well. However, since wellbore lengths and layer thicknesses may be different in each layer, the geometrical pseudo-skin  $S_{gj}$  is also different in each layer. Therefore, the use of late-time data to determine the mechanical damage from the equivalent total skin factor is quite challenging, and out of the scope of this work.

### 3 Proposed Methods for Estimating Layer Properties

Eqs. (1) and (7) may also be applied for a given layer  $j$ . Thus, at early-times, pressure change in layer  $j$  may be approximated by:

$$\Delta p_{wf}(t) = \frac{q_j(t)B\mu_j}{k_{zxj}L_j} \left[ \frac{1}{2} \ln \left( \frac{4k_{zxj}t}{\exp(\gamma)\phi_j\mu_j c_{tj}r_w^2} \right) + S_j \right]. \quad (14)$$

The late-time logarithm approximation for pressure change in layer  $j$ , in its turn, is given by:

$$\Delta p_{wf}(t) = \frac{q_j(t)B\mu_j}{k_{xyj}h_j} \left[ \frac{1}{2} \ln \left( \frac{4k_{xyj}t}{\exp(\gamma)\phi_j\mu_j c_{tj}r_w^2} \right) + S_{tj} \right]. \quad (15)$$

To obtain Eqs. (14) and (15), it was assumed that wellbore pressure is the same in all layers, except for the hydrostatic column. Furthermore, it was considered that the durations of early- and late-time radial flow have been previously identified from pressure derivative data. It is also important to highlight here that, in Eqs. (14) and (15), layer flow-rate  $q_j$  is a function of time. As explained in Appendix A, flow-rates are updated at each time step and, therefore, may change in time (Pan et al., 2010).

Based on Eqs. (14) and (15), the RNPA (Ehlig-Economides and Joseph, 1987; Raghavan, 1989) and DTM (Galvão and Guimarães, 2017; Guimarães and Galvão, 2017) were extended to multilayer systems with multilateral horizontal wells, as the schematic portrayed in Fig. 1.

#### 3.1 Rate-Normalized Pressure Analysis

Rate-normalized pressure change is defined as the ratio between wellbore pressure and the instant flow-rate at a given time (Ehlig-Economides and Joseph, 1987; Raghavan, 1989). Starting from Eq. (14), the rate-normalized pressure change in layer  $j$  during early-time radial flow may be computed as:

$$p_{Nj}(t) = \frac{\Delta p_{wf}(t)}{q_j(t)} = \frac{B\mu_j}{k_{zxj}L_j} \left[ \frac{1}{2} \ln \left( \frac{4k_{zxj}t}{\exp(\gamma)\phi_j\mu_j c_{tj}r_w^2} \right) + S_j \right]. \quad (16)$$

The rate-normalized pressure analysis (RNPA) encompasses the changes in pressure and layer flow-rate into a single function of time. Therefore, it is more suitable for estimating individual layer permeabilities than merely the pressure data. Eq. (16) shows that the rate-normalized pressure change behaves as a linear function of the natural logarithm of time. Taking the derivative of Eq. (16) with respect to the natural logarithm of time:

$$\frac{\partial p_{Nj}(t)}{\partial \ln(t)} = m_{erfj} = \frac{B\mu_j}{2k_{zxj}L_j} \quad \longrightarrow \quad k_{zxj} = \frac{B\mu_j}{2m_{erfj}L_j}. \quad (17)$$

Thus, layer permeabilities in the  $zx$ -plane may be obtained from Eq. (17), using the rate-normalized pressure data corresponding to the early-time radial flow. The mechanical skin factor in layer  $j$ , then, may be estimated as:

$$S_j = \frac{1}{2} \left[ \frac{p_{Nj}(t_{erf})}{m_{erfj}} - \ln(t_{erf}) - \ln \left( \frac{4k_{zxj}}{\exp(\gamma)\phi_j\mu_j c_{tj}r_w^2} \right) \right], \quad (18)$$

where  $t_{erf}$  and  $p_{Nj}(t_{erf})$  represent, respectively, an arbitrary time point during which early-time radial flow is observed and the corresponding rate normalized pressure change in layer  $j$ .

At late-times, an expression for the rate-normalized pressure change may be obtained from Eq. (15):

$$p_{Nj}(t) = \frac{\Delta p_{wf}(t)}{q_j(t)} = \frac{B\mu_j}{k_{xyj}h_j} \left[ \frac{1}{2} \ln \left( \frac{4k_{xyj}t}{\exp(\gamma)\phi_j\mu_j c_{tj}r_w^2} \right) + S_{tj} \right]. \quad (19)$$

The horizontal permeability in layer  $j$  may be estimated from the derivative of Eq. (19) with respect to the natural logarithm of time:

$$\frac{\partial p_{Nj}(t)}{\partial \ln(t)} = m_{lrfj} = \frac{B\mu_j}{2k_{xyj}h_j} \longrightarrow k_{xyj} = \frac{B\mu_j}{2m_{lrfj}h_j}. \quad (20)$$

Thus, for a given time point  $t_{lrf}$  such that late-time radial flow occurs, and its corresponding rate normalized pressure change  $p_{Nj}(t_{lrf})$ , total skin factor in layer  $j$  may also be computed by:

$$S_{tj} = \frac{1}{2} \left[ \frac{p_{Nj}(t_{lrf})}{m_{lrf}} - \ln(t_{lrf}) - \ln \left( \frac{4k_{xyj}}{\exp(\gamma)\phi_j\mu_j c_{tj}r_w^2} \right) \right]. \quad (21)$$

### 3.2 Delta Transient Method

The application of the RNPA presents an intrinsic operational drawback, which is the need to continuously measure layer flow-rates. To overcome this issue, Galvão and Guimarães (2017) and Guimarães and Galvão (2017) derived an alternative proposal to estimate individual layer permeabilities and skin factors. They referred to their method as the Delta Transient Method (DTM). Their motivation to develop this procedure was to avoid the need of registering layer flow-rates several times. This section presents an extension of the DTM to multilayer reservoirs with multilateral horizontal wells.

Based on the early-time logarithmic approximation for pressure change in layer  $j$ , given by Eq. (14), two variables  $\delta_{erfj}$  and  $\beta_j(t)$  shall be defined as follows:

$$\delta_{erfj} = \ln(k_{zxj}) + 2S_j; \quad \beta_j(t) = \ln \left( \frac{4t}{\exp(\gamma)\phi_j\mu_j c_{tj}r_w^2} \right). \quad (22)$$

Thus, replacing Eq. (22) in Eq. (14):

$$\Delta p_{wf}(t) = \frac{q_j(t)B\mu_j}{2k_{zxj}L_j} [\beta_j(t) + \delta_{erfj}]. \quad (23)$$

Rearranging Eq. (23) in a more convenient way:

$$\frac{2k_{zxj}L_j}{B\mu_j} = \frac{q_j(t) [\beta_j(t) + \delta_{erfj}]}{\Delta p_{wf}(t)}. \quad (24)$$

One should note that no further assumption was made to obtain Eq. (24), expect for those already mentioned in Section 2 and Appendix A. It requires only the logarithmic approximation given by Eq. (14) to be valid. Thus, for two distinct time points  $t_1$  and  $t_2$  during which early-time radial flow regime is occurring:

$$\frac{q_j(t_1) [\beta_j(t_1) + \delta_{erfj}]}{\Delta p_{wf}(t_1)} = \frac{2k_{zxj}L_j}{B\mu_j} = \frac{q_j(t_2) [\beta_j(t_2) + \delta_{erfj}]}{\Delta p_{wf}(t_2)}, \quad (25)$$

which implies that:

$$\delta_{erfj} \frac{q_j(t_1)}{\Delta p_{wf}(t_1)} + \frac{q_j(t_1)\beta_j(t_1)}{\Delta p_{wf}(t_1)} = \delta_{erfj} \frac{q_j(t_2)}{\Delta p_{wf}(t_2)} + \frac{q_j(t_2)\beta_j(t_2)}{\Delta p_{wf}(t_2)}. \quad (26)$$

Therefore, isolating  $\delta_{erfj}$ :

$$\delta_{erfj} = \frac{\left( \frac{q_j\beta_j}{\Delta p_{wf}} \right) \Big|_{t=t_2} - \left( \frac{q_j\beta_j}{\Delta p_{wf}} \right) \Big|_{t=t_1}}{\left( \frac{q_j}{\Delta p_{wf}} \right) \Big|_{t=t_1} - \left( \frac{q_j}{\Delta p_{wf}} \right) \Big|_{t=t_2}}. \quad (27)$$

Thus,  $\delta_{erfj}$  may be determined from Eq. (27). Then, the vertical permeability in layer  $j$  is estimated from Eq. (23):

$$k_{zxj} = \frac{q_j(t)B\mu_j}{2L_j\Delta p_{wf}(t)} [\beta_j(t) + \delta_{erfj}]. \quad (28)$$

Moreover, the mechanical skin  $S_j$  is evaluated from the definition of  $\delta_{erfj}$ :

$$S_j = \frac{\delta_{erfj} - \ln(k_{zxj})}{2}. \quad (29)$$

An analogous procedure may be applied using late radial flow data. The definition of  $\delta$ , now, should be given by:

$$\delta_{lrfj} = \ln(k_{xyj}) + 2S_{tj}. \quad (30)$$

Then, similar computations show that the total skin factors and horizontal permeabilities in each layer may be obtained from late-time data:

$$\delta_{lrfj} = \frac{\left(\frac{q_j\beta_j}{\Delta p_{wf}}\right)\Big|_{t=t_4} - \left(\frac{q_j\beta_j}{\Delta p_{wf}}\right)\Big|_{t=t_3}}{\left(\frac{q_j}{\Delta p_{wf}}\right)\Big|_{t=t_3} - \left(\frac{q_j}{\Delta p_{wf}}\right)\Big|_{t=t_4}}. \quad (31)$$

In Eq. (31),  $t_3$  and  $t_4$  denote two distinct time points after late-time radial flow has already started. Thus, horizontal permeability in layer  $j$  is determined as follows:

$$k_{xyj} = \frac{q_j(t)B\mu_j}{2h_j\Delta p_{wf}(t)} [\beta_j(t) + \delta_{lrfj}]. \quad (32)$$

Total skin factor is evaluated from the definition of  $\delta_{lrfj}$ :

$$S_{tj} = \frac{\delta_{lrfj} - \ln(k_{xyj})}{2}. \quad (33)$$

### 3.3 Reasonableness Check

Galvão and Guimarães (2017) claimed that a reasonableness check must be performed to assess if the computed layer properties are consistent with the estimated reservoir equivalent parameters. The reasonableness check consists of comparing the reservoir equivalent properties obtained from conventional drawdown/buildup analysis with the computed properties for each individual layer. If the difference between these results is relevant, then the assumptions made in the development of RNPA and DTM (such as the logarithmic approximations for pressure change) are not valid (Galvão and Guimarães, 2017; Guimarães and Galvão, 2017). In that case, the estimates for individual layer parameters should be discarded.

In this work, we propose that the values for layer permeabilities evaluated from both the RNPA and the DTM should be applied in Eqs. (2) and (8) to compute the reservoir equivalent permeabilities. These equivalent permeabilities should be compared to the reservoir equivalent permeabilities determined from Eqs. (5) and (12).

Besides, the mechanical skin factors determined from early-time data should be applied in Eq. (4) and compared to the equivalent mechanical skin obtained from Eq. (6). Conventional pressure interpretation methods do not allow the determination of an equivalent mechanical skin based on late-time radial flow data, due to the pseudo-skin factor in each layer. Thereby, the reasonableness check for late-time skin factors should be performed using total skins, instead of the mechanical skin. Thus, the obtained estimates for  $S_{tj}$  should be applied in Eq. (9) and compared to the value of  $S_{teq}$  computed from Eq. (13).

As stated by Guimarães and Galvão (2017), if the equivalent properties computed from the estimated individual layer properties are significantly different from those obtained from the conventional analysis, then the results should be discarded. In their work, Guimarães and Galvão (2017) did not provide a more objective criteria to assess the result of the reasonableness check. In this

work, the maximum acceptable difference between the equivalent parameters was set as 10%. This means that, if the estimated layer properties yield equivalent permeabilities and skin factors that are 10% higher (or lower) than the values obtained from conventional analysis, then the results should not be considered.

### 3.4 Nelder-Mead Simplex Algorithm

Application of the RNPA and DTM requires the constant derivative levels related to early- and late-time radial flow to be clearly identified. Otherwise, the logarithmic approximations given by Eqs. (14) and (15) are not valid. However, depending on layer thicknesses and wellbore laterals lengths, early-time radial flow may end so quickly that no constant derivative level is identified (Odeh and Babu, 1990; Kuchuk et al., 1991). Identification of early-time radial flow is also compromised if the wellbore storage effect is relevant. Besides, if the wellbore is significantly long, late-time radial flow may not be observed during the test (Ozkan et al., 1989; Rosa and Carvalho, 1989).

Therefore, optimization methods represent an interesting alternative to estimate layer parameters, since they do not rely on the identification of any flow regime. The Nelder-Mead simplex algorithm (NM) is a gradient-free global optimization procedure that is based on simply evaluating the objective function at the vertices of a simplex (Nelder and Mead, 1965; Feng et al., 2020). The simplex is defined as a set of  $N + 1$  vertices, where  $N$  is the number of independent variables of the objective function. Then, the vertex that yields the highest objective function value is successively replaced until a convergence criteria is satisfied (Luersen and Le Riche, 2004; Barati, 2011).

At each iteration, there are four possible operations that determine how the simplex should be updated: reflection, expansion, contraction and shrinkage. Then, after the proper operation is performed, a new simplex is generated and convergence is checked. If the convergence criteria is satisfied, the algorithm stops. Otherwise, a new iteration is performed (Ghiasi et al., 2007; Rahmati et al., 2013). A more detailed flow-chart of Nelder-Mead algorithm is given in Appendix B.

Layer permeabilities in the horizontal plane and in the  $z$ -direction were set as model parameters, as well as their respective skin factors. Therefore, the vector of model parameters  $x$  was defined as:

$$x = \{k_{xy1}, k_{xy2}, \dots, k_{xyn}, k_{z1}, k_{z2}, \dots, k_{zn}, S_1, S_2, \dots, S_n\}. \quad (34)$$

Layer porosities, wellbore lateral lengths, layer thicknesses and rock and fluid compressibilities are assumed to be constant and known. For this reason, they were not considered as model parameters to be determined by the method. It was assumed that pressure and layer flow-rates were measured at  $N_{me}$  times. Thus, the objective function to be minimized was defined as:

$$O(x) = \frac{\|p_{wf}^{obs} - p_{wf}(x)\|_2}{\|p_{wf}^{obs}\|_2} + \sum_{j=1}^n \frac{\|q_j^{obs} - q_j(x)\|_2}{\|q_j^{obs}\|_2}, \quad (35)$$

where  $\|p_{wf}^{obs}\|_2$  is the Euclidean norm of the  $N_{me}$ -dimensional vector that contains the observed pressure data at all time steps,  $\|p_{wf}^{obs} - p_{wf}(x)\|_2$  is the Euclidean norm of the  $N_{me}$ -dimensional vector that represents the mismatch between the observed pressure and the pressure data estimated using vector  $x$  of model parameters,  $\|q_j^{obs}\|_2$  is the Euclidean norm of the  $N_{me}$ -dimensional vector that contains the observed flow-rate data in layer  $j$  at all time steps and  $\|q_j^{obs} - q_j(x)\|_2$  is the Euclidean norm of the  $N_{me}$ -dimensional vector that represents the mismatch between the observed flow-rates in layer  $j$  and the flow-rate profile for layer  $j$  computed using vector  $x$  of model parameters.

The objective function given in Eq. (35) is expected to present a unique minimum. Moreover, in a theoretical case where pressure and flow-rate measurements are free of noise and errors, the objective function definition will imply that  $O(x) = 0$ . Field data, however, are always subject to noise. Therefore, even if the vector of model parameters  $x$  matches the true parameter values, some mismatches between computed and observed data will occur, and the objective function will be non-zero. Nonetheless, since the objective function defined in Eq. (35) accounts for both pressure and flow-rate data, it is expected to have a unique or acceptable local minimum.

$q$ (m <sup>3</sup> /d)	$\mu$ (cP)	$c_r$ (kgf/cm <sup>2</sup> ) <sup>-1</sup>	$c_o$ (kgf/cm <sup>2</sup> ) <sup>-1</sup>	$B$ (m <sup>3</sup> /m <sup>3</sup> std)
2000	3.1	8.0x10 <sup>-5</sup>	1.14x10 <sup>-4</sup>	1.0

Table 1: Input Reservoir Parameters

The convergence criteria was set based on the decrease of the objective function. At each iteration, the simplex vertex that presents the highest objective function values is replaced. Therefore, it is expected that, at each iteration, the maximum objective function value presented by the new simplex decreases. If the absolute difference between the objective function maximum value considering all simplex vertices is significantly small after two successive iterations, then further iterations will not improve the estimates for model parameters. In this work, we established that if the absolute difference between objective function maximum value after two successive iterations is smaller than  $1 \times 10^{-15}$ , then converged was reached.

NM was originally proposed for unconstrained optimization (Nelder and Mead, 1965). Therefore, if no restrictions are applied, the algorithm may eventually generate a simplex with negative values for layer permeability, which does not make physical sense. It is possible, however, to impose boundary constraints to the algorithm (Ghiasi et al., 2007). A simple constraint consists of defining a range that should contain the estimated parameters. This kind of linear boundary constraint is easily coupled to the NM work-chart depicted in appendix B by checking, at each iteration, if all members of the updated simplex are within the determined range. In this work, the linear boundary constraints were applied to NM algorithm as described by Luersen and Le Riche (2004).

Recalling Eq. (34), layer permeabilities and skin factors were set as model parameters. For each layer, the permeability lower limit was set as 10 mD and the upper limit was set as 1000 mD. In all cases, both horizontal and vertical permeabilities for the initial simplex were randomly chosen inside this range. Initial skin factors, in their turn, consisted of randomly chosen values between -1.0 and 8.0.

#### 4 Results

The techniques described in Section 3 to estimate individual layer properties were applied at a pair of synthetic cases to assess their accuracy. Production flow-rate, oil viscosity and rock and oil compressibilities were the same in both cases. The values are reported in Table 1. Layer properties in each case are displayed in Table 2. Effective wellbore lengths, layer porosities, compressibilities and the distances between wellbore laterals and a reservoir vertical boundary were assumed to be known. A production period of 480 hours (20 days) was considered. This test time was long enough for the late-time radial flow regime to develop in both cases. No boundary effects are observed, because the reservoir was assumed to be laterally infinite.

Figure 2 shows the reference pressure and pressure derivative data for both cases, while Figure 3 exhibits the reference flow-rate data. In each case, the reference data consists of 61 distinct pressure points and 61 flow-rate measurements per layer. Data shown in Figures 2 and 3 were computed using the analytical model developed by Pan et al. (2010), as detailed in Appendix A.

Case	$\phi_j$	$h_j$ (m)	$dz_j$ (m)	$L_j$ (m)	$k_{xyj}$ (mD)	$k_{zj}$ (mD)	$k_{zxj}$ (mD)	$S_j$
A	0.16	20	10.0	700	350	350	350	4.1
	0.30	20	10.0	800	480	480	480	2.1
	0.23	25	12.5	600	570	570	570	6.1
B	0.24	20	10.0	600	600	300	424	3.3
	0.30	15	7.5	500	500	250	354	4.8

Table 2: Layer Properties in Each Case

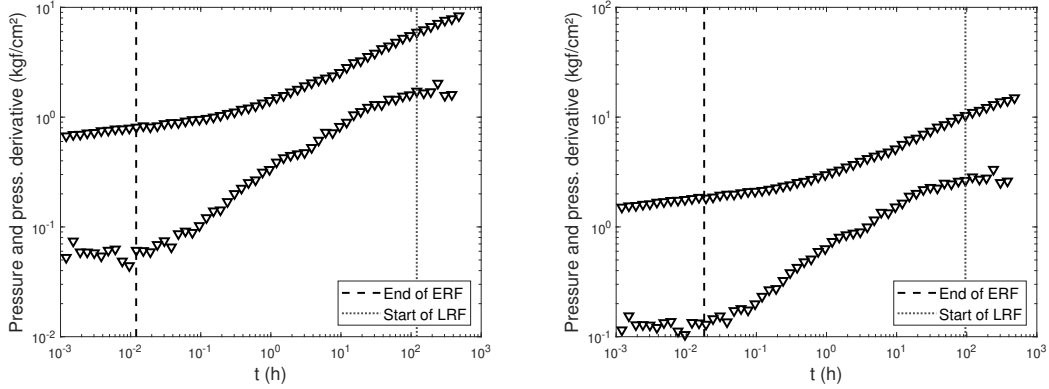


Fig. 2: Reference pressure and derivative data for cases A (left) and B (right)

To represent a more realistic condition, an artificial noise was added to the computed pressure and flow-rate data. Flow-rate noise consisted of a Gaussian noise with mean zero and a standard deviation equal to 1% of the noise-free flow-rate in each layer. The pressure noise, in its turn, presents two components: one sinusoidal term and one Gaussian term. The sinusoidal term, which represents a tidal effect, has amplitude equal to 1% of the maximum true pressure data. The Gaussian term presents mean zero and standard deviation equal to 0.1% of the maximum true pressure data.

In a real case, higher measurement errors may be observed. However, as stated in Section 3, the application of the RNPA and DTM requires that the constant derivative levels associated with early- and late-time radial flow are clearly identified. For this reason, the artificial noise was set with a relatively small amplitude, so that constant derivative levels may still be clearly identified.

All three methods were applied considering the noisy pressure and flow-rate data shown in Figures 2 and 3. Since wellbore lengths and reservoir properties are different in each case, early- and late-time radial flow occur at distinct time ranges (Ozkan et al., 1989; Odeh and Babu, 1990). The vertical dashed lines in Figure 2 indicate the moment when early-time radial flow ends, while the dotted vertical lines represent the start of late-time radial flow regime.

Hence, the early-time logarithmic approximations presented in Eqs. (1) and (14) are valid for all times before the vertical dashed lines, whereas the late-time approximations given by Eqs. (7) and (15) are applicable for all times after the dotted vertical lines in Figure 2. In other words, it was assumed that early-time radial flow is simultaneously occurring in all layers until the moment

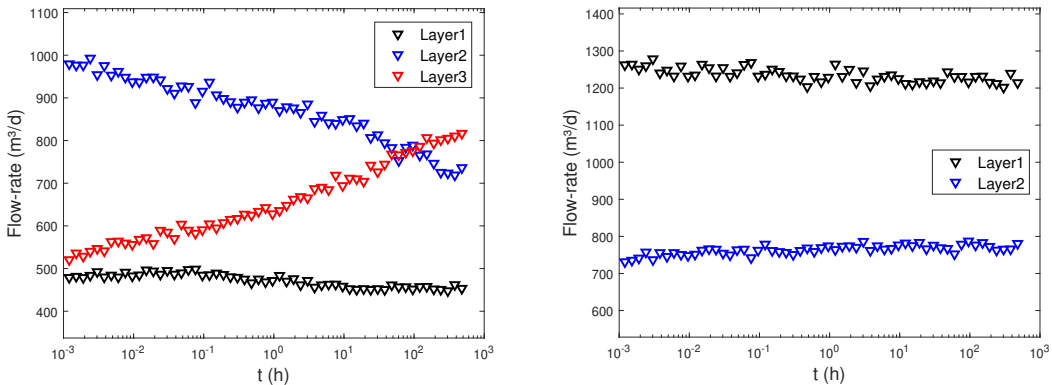


Fig. 3: Reference flow-rate data for cases A (left) and B (right)

Case	$(k_{zx})_{eq}$ (mD)	$S_{eq}$	$(k_{xy})_{eq}$ (mD)	$S_{teq}$
A	464	2.11	520	-7.56
B	413	2.50	605	-7.28

Table 3: Estimated reservoir equivalent properties

signed with a vertical dashed lines (and analogously with late-time radial flow and the vertical dotted lines).

NM, in its turn, aims to match pressure and flow-rate data for the entire test time according to the objective function defined in Eq. (35). For this reason, NM does not require a clear identification of any specific flow regime. As mentioned in Section 3.4, the initial simplex is built by randomly sorted values within a determined range. Thus, the Nelder-Mead algorithm was performed five times for each case to assure that the algorithm converges to the same set of properties even if the initial simplex is changed. At each run, different initial guesses were used. The initial simplex parameters in each run consisted of randomly sorted values with uniform distribution. As mentioned in Section 3.4, linear constraints for the NM algorithm were specified. The minimum layer permeability value was set as 10 mD, whereas the maximum layer permeability value was set as 1000 mD. As for the layer mechanical skin factors, it was considered a range between -1.0 and 8.0. Differences between estimated layer properties for each trial were smaller than 1%. These results evidence that the initial guesses for NM did not affect the method convergence towards the unique global minimum. In this section, results for the first trial are reported.

Conventional pressure transient analysis depicted in Section 2 was performed to estimate the reservoir equivalent parameters. Thus, the reference pressure and pressure derivative data displayed in Figure 2 were used to determine the reservoir equivalent permeabilities (as indicated in Eqs (5) and (12)) and the reservoir mechanical and total equivalent skin factors (as mentioned in Eqs. (6) and (13)). The obtained results, which may be observed in Table 3, are relevant due to the reasonableness check that must be performed to assess the consistency of estimated layer parameters. As described in in Section 3.3, if layer properties are successfully estimated, then the parameters displayed in Table 3 must be close to the equivalent reservoir properties obtained by RNPA and DTM.

As explained in Section 2, at late-times, the stream lines convergence becomes relevant, inducing a pseudo-skin beside the mechanical damage around the wellbore (Daviau et al., 1988; Kuchuk et al., 1991; Yildiz, 2003). Stream lines convergence may occur differently in each layer, making it unfeasible to tell apart the pseudo and mechanical skin effects during late-time radial flow in multilayer reservoirs. For this reason, the equivalent skin computed using late-time radial flow data represents a total equivalent skin, as defined in Eqs. (9) and (10). Estimates for the equivalent mechanical skin factor as defined in Eq. (4) were computed using early-time radial flow data only.

Table 4 displays, for each case, the objective function values considering the true model parameters and the estimated layer properties obtained by the NM method. Estimates for the permeability in  $z$ -direction ( $k_{zj}$ ) are also shown. It is interesting to notice that the estimated parameters yielded a lower objective function value than the true set of layer properties, which may be explained by the artificial noise added to the observed data. Estimates for  $k_{zj}$  presented a significant error in

Case	$O(x_{true})$	$O(x_{est})$	$k_{zj}$ (mD)		
			True	Est.	Err. (%)
A	0.0496	0.0475	350	341	-2.4
			480	461	-4.0
			570	512	-10.1
B	0.0324	0.0313	300	267	-10.9
			250	214	-14.4

Table 4: Objective function values at the final iteration of the NM method, objective function values considering the vector of true model parameters and estimated values of  $k_{zj}$  in each layer

Case	True	RNPA		DTM		NM	
		Est.	Err. (%)	Est.	Err. (%)	Est.	Err. (%)
A	350	372	6.4	308	-12.1	346	-1.3
	480	460	-4.2	516	7.4	471	-1.8
	570	678	19.0	604	6.0	544	-4.6
B	424	427	0.6	418	-1.6	401	-5.4
	354	385	9.0	399	13.0	329	-7.0

Table 5: Estimated vertical permeabilities ( $k_{zxj}$ ) in each layer (permeabilities in mD)

case B. However, it is more meaningful to analyze the estimated permeabilities in the vertical plane ( $k_{zxj}$ ) rather than the permeabilities in  $z$ -direction.

Tables 5 and 6 show the estimated values for layer permeability in the  $zx$ -plane and mechanical skins, respectively. One should recall that the layer permeability in the  $zx$ -plane ( $k_{zxj}$ ) is not directly estimated by the NM method, since only layer permeabilities in the  $z$ -direction and in the  $xy$ -plane were set as model parameters. Table 5 shows the geometric mean of the values for  $k_{zj}$  and  $k_{xyj}$  computed by the NM algorithm, to make the comparison with the RNPA and DTM easier. Analogously to the conventional analysis, estimates for  $k_{zxj}$  and  $S_j$  using RNPA and DTM in Table 6 consider early-time data only, as outlined in Sections 2, 3.1 and 3.2. Skin factors computed from the NM algorithm, on the other hand, use data from the entire test, since this method does not rely on the identification of any flow regime.

As evidenced by Table 5, the three methods yielded good estimates for layer permeabilities. Given that result, one should notice that the RNPA and DTM are much easier to implement than the NM method. Provided that early- and late-time radial flow regimes have been properly identified, the 2 techniques based on logarithmic approximations demand only a general worksheet software to be performed. The NM method, in its turn, requires not only a computational implementation of the analytical solution proposed by Pan et al. (2010), but also regular flow-rate measurements during the test. The simpler implementation of the RNPA and DTM, however, explains the higher errors observed in some cases (for instance, the estimated permeability of layer 3 using RNPA), since less data are used by these methods. Thus, the results were acceptable considering the trade-off between simplicity and accuracy, and that the techniques based on the logarithmic approximations use only part of the pressure and flow-rate history, whereas the NM algorithm uses data from the entire test.

Even though layer permeabilities were well estimated, Table 6 shows that only the NM method was able to provide accurate estimates for layer mechanical skin factors. This is possibly explained by the fact that the two methods based on logarithmic approximations are more sensitive to data measurement errors (represented by the artificial noise) than the NM algorithm. As evidenced by Eq. (18), layer skin factors are estimated by the RNPA using the pressure and flow-rate data at only one point (in this work, layer skin factors were estimated considering pressure and flow-rate data at  $t = 0.006$  h). DTM, in its turn, depends on data at two distinct time points, as explained in Section 3.2. Therefore, the two methods based on logarithmic approximations are more sensitive to measurement errors, despite being much simpler than the NM algorithm.

Comparing the results in Tables 5 and 6, it is also interesting to notice errors magnitude considering RNPA and DTM were similar. As detailed by Galvão and Guimarães (2017), the need to repeatedly measure layer flow-rates consists of a significant operational setback of RNPA. On the other hand, DTM requires PLT data from only 2 distinct time steps during early-time radial flow

Case	True	RNPA		DTM		NM	
		Est.	Err. (%)	Est.	Err. (%)	Est.	Err. (%)
A	4.1	2.9	-29.2	1.7	-57.1	4.1	1.2
	2.1	1.0	-54.7	1.5	-31.0	2.1	0.9
	6.1	5.1	-16.6	4.4	-28.2	5.9	-4.1
B	3.3	2.0	-39.6	1.7	-46.4	3.0	-7.4
	4.8	3.5	-26.2	3.8	-20.4	4.3	-9.2

Table 6: Estimated mechanical skin factors ( $S_j$ ) in each layer

Case	True	RNPA		DTM		NM	
		Est.	Err. (%)	Est.	Err. (%)	Est.	Err. (%)
A	350	399	13.9	396	13.1	350	-0.1
	480	573	19.4	478	-0.4	482	0.4
	570	610	7.0	546	-4.2	578	1.4
B	600	657	9.5	657	9.4	603	0.5
	500	556	11.2	479	-4.1	505	1.1

Table 7: Estimated horizontal permeabilities ( $k_{xyj}$ ) in each layer (permeabilities in mD)

and 2 time steps during late-time radial flow. Therefore, results from tables 5 and 6 indicate that the DTM is preferable to RNPA, since both yielded estimates for layer properties with similar accuracy.

Table 7 exhibits the estimated horizontal permeabilities for all three methods. Permeabilities from RNPA and DTM were determined using late-time data, while NM estimates were computed considering pressure and flow-rates profiles during the entire test. Results show a decent accuracy, expect for the RNPA in case A. This is possibly related to the sinusoidal component of the artificial noise added to the pressure data. This oscillatory component is more relevant at late-times and, therefore, directly impacts the horizontal permeability estimates. Nonetheless, both the DTM and the NM algorithm were able to provide good estimates for layer permeabilities. Moreover, comparing Tables 5 and 7, the estimated layer permeabilities indicate that anisotropy effects are substantially more pronounced in case B than in case A, which is expected, since case A consists of a isotropic reservoir.

One should notice that NM only provides one estimate for the mechanical skin in each layer, as it attempts to find a set of parameters that fit pressure and flow-rate data during the entire test. In contrast, the RNPA and DTM allow determination of layer total skin factors ( $S_{tj}$ ) from late-time radial flow data. Then, an alternative estimate for the mechanical skins in each layer may be computed from Eqs. (10) and (11). Estimates for layer total and mechanical skin factors computed from late-time data are reported in Table 8.

In both cases, total skin factor for each layer was determined with decent accuracy. However, errors were hugely magnified when the estimated total skin factors were applied in Eq. (10) to evaluate the mechanical skin in each layer. These results show that the mechanical skin computation based on late-time radial data is highly sensitive to errors in the determination of total skin factors. As defined in Eqs. (10) and (11), estimates for both horizontal and vertical permeabilities and total skin factors are required to obtain the mechanical skin from late-time radial flow data. Therefore, computation of the mechanical skin is influenced by the accuracy of three other estimated properties, specially the total skin factor. Moreover, the ratio between layer wellbore length and thickness also magnifies the errors from total skin estimates.

In Section 3.3, it was stated that a reasonableness check must be performed to verify if estimated layer parameters are consistent with the reservoir equivalent properties (Galvão and Guimarães, 2017; Guimarães and Galvão, 2017), which are determined through conventional pressure analysis techniques. Thus, for each method, estimated layer properties were applied in Eqs. (2), (4), (8) and (9) and compared to the equivalent properties reported in Table 3, which were estimated from the pressure profiles and using Eqs. (5), (6), (12) and (13). As mentioned in Section 3.3,

Case	Total skin ( $S_{tj}$ )					Mechanical skin ( $S_j$ )				
	True	RNPA		DTM		True	RNPA		DTM	
		Est.	Err. (%)	Est.	Err. (%)		Est.	Err. (%)	Est.	Err. (%)
A	-7.52	-7.51	-0.1	-7.56	0.6	4.1	4.3	4.7	2.5	-38.6
	-7.73	-7.67	-0.7	-7.85	1.7	2.1	4.3	104	-3.0	-240
	-7.16	-7.35	2.7	-7.58	5.8	6.1	1.6	-74.4	-3.8	-162
B	-7.26	-7.32	0.8	-7.36	1.4	3.3	2.0	-38.7	1.1	-67.1
	-7.05	-7.16	1.5	-7.38	4.6	4.8	2.3	-50.7	-2.9	-160.2

Table 8: Estimates for total skin factors ( $S_{tj}$ ) and mechanical skin factors ( $S_j$ ) in each layer using late-time radial flow data

Case	Property	Conv. An.	RNPA		DTM		NM	
			Estim.	Diff. (%)	Estim.	Diff. (%)	Estim.	Diff. (%)
A	$(k_{zx})_{eq}$	452	493	8.5	472	3.8	450	-0.9
	$S_{eq}$	2.00	3.08	54.1	2.60	30.3	3.92	96.5
	$(k_{xy})_{eq}$	520	534	2.6	479	-7.9	478	-8.1
	$S_{teq}$	-7.56	-7.50	-0.8	-7.66	1.3	N/A	
B	$(k_{zx})_{eq}$	403	408	1.2	409	1.6	368	-8.6
	$S_{eq}$	2.37	2.63	11.0	2.65	12.0	3.54	49.6
	$(k_{xy})_{eq}$	605	614	1.5	581	-4.0	561	-7.2
	$S_{teq}$	-7.28	-7.25	-0.4	-7.37	1.1	N/A	

Table 9: Reasonableness check for both cases (permeabilities in mD)

the reasonableness check is particularly important to assess the results obtained through RNPA and DTM, since these techniques rely on the validity of the logarithmic approximations given by Eqs. (14) and (15). Furthermore, it was also assumed that early- and late-time radial flow simultaneously occur in all layers considering the time ranges defined by the vertical lines of Figure 2. NM application, however, requires only that the analytical formulation developed by Pan et al. (2010) is valid. Therefore, the acceptance criteria of maximum 10% difference proposed in Section 3.3 was applied only at RNPA and DTM.

Equivalent mechanical skins for RNPA and DTM were computed using the early-time estimates for layer skin factors because the late-time estimates presented higher errors (as displayed in Tables 6 and 8). Furthermore, isolating an equivalent mechanical skin from the total equivalent skin factor evaluated during late-time radial flow is a complicated task. Thus, the reasonableness check for skin factors computed from late-time data should be performed with respect to total skin factors, rather than mechanical skins. Since the NM algorithm does not provide direct estimates for total skin factors, no reasonableness check was performed regarding the total skin factors for NM.

The reasonableness checks are exhibited in Table 9. For both RNPA and DTM the estimated layer properties provided equivalent reservoir permeabilities and total skin factors are very close to the values obtained by conventional analysis, and should be considered valid according to the maximum acceptable difference established in Section 3.3.

Nonetheless, the equivalent mechanical skin factors evaluated by RNPA and DTM presented significant differences compared to the values obtained by conventional analysis. These results are an immediate consequence of the poor layer mechanical skin estimates, reported in Table 6. In summary, the reasonableness checks endorse the accuracy of estimated layer permeabilities for all methods, but evidenced that the techniques based on logarithmic approximations failed to provide good estimates for layer mechanical skins.

Equivalent permeabilities computed using the individual layer permeabilities obtained from NM were also close to values determined through conventional analysis. However, interestingly enough, the NM equivalent mechanical skins also presented relevant differences despite the fact that this technique provided good estimates for individual layer skin factors (as shown in Table 6). This result is possibly explained by the artificial noise added to the pressure data. The equivalent mechanical skin is determined through Eq. (13) and, thus, is also sensitive to pressure measurement errors.

A final accuracy assessment was performed by comparing the reference pressure and flow-rate data to the pressure and flow-rate profiles computed by applying the layer properties estimated by each method into the analytical model developed by Pan et al. (2010). Figure 4 shows the comparison between pressure and pressure derivative profiles for each method and the reference data, while Figure 5 displays the comparison between flow-rate profiles. The NM method is the only technique that aims to fit layer flow-rate data, according to the objective function defined in Eq. (35). Therefore, Figure 5 compares the reference flow-rate data only to the flow-rate data obtained using the parameters determined by the NM method. In Figure 4, RNPA and DTM pressure data were computed considering that layer skin factors are equal to the values portrayed in Table 6. That is, estimates for skin factors obtained from early-time data were used to determine the pressure profile.

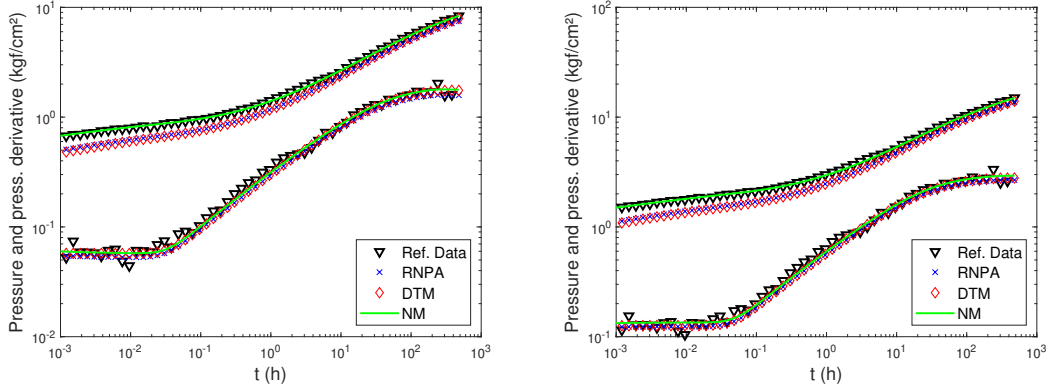


Fig. 4: Comparison between estimated and reference pressure data for cases A (left) and B (right)

A good agreement is observed between reference pressure derivative data and the pressure derivative profiles computed using the estimated layer properties for all methods. Pressure derivative reflects the reservoir equivalent permeability (Larsen, 1982; Ehlig-Economides and Joseph, 1987; Galvão and Guimarães, 2017). Therefore, the good agreement between pressure derivative curves observed in Figure 4 endorses that layer permeabilities were accurately estimated by all methods.

Pressure change, in its turn, is also affected by layer skin factors. Pressure change curves computed using the parameters obtained by the RNPA and DTM are slightly lower than the reference data. The NM pressure data, on the other hand, presented a great agreement with the reference data. These differences, combined with the pressure derivative profiles, suggest that only the NM algorithm provided good estimates for layer skin factors, which is consistent with the comparison between estimated layer mechanical skins shown Table 6.

Finally, Figure 5 shows an excellent match between the reference data and layer flow-rate profiles obtained using the parameters estimated by the NM method. This great match endorses the accuracy of the NM algorithm.

As previously mentioned, the NM algorithm does not rely on the identification of any specific flow regime. To verify its performance in cases where early- or late-time radial flow are not clearly identified, the NM method was applied two other times in case A, discarding part of the reference pressure and flow-rate data. First, data for  $t > 100$  h were discarded, to represent a case where only

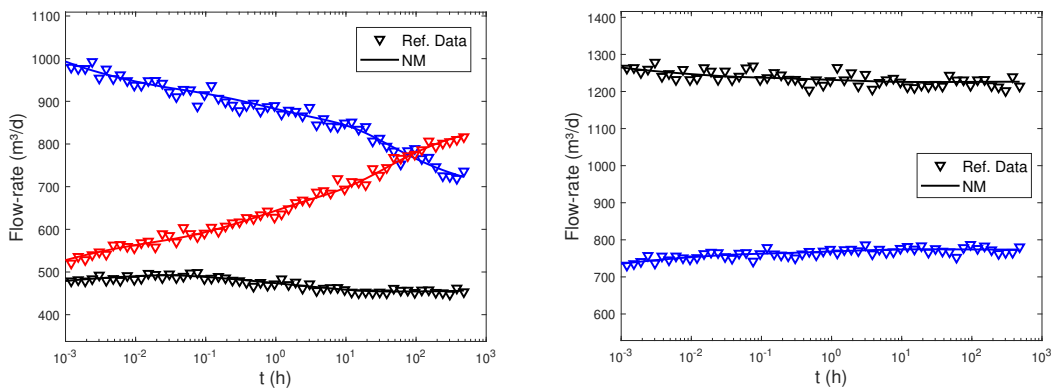


Fig. 5: Comparison between estimated and reference flow-rate data for cases A (left) and B (right): Layer 1 is represented in black, layer 2 is represented in blue and layer 3 is represented in red

$O(x)$		$k_{xyj}$ (mD)			$k_{zj}$ (mD)			$k_{zxj}$ (mD)			$S_j$		
True	Est.	True	Est.	Err.	True	Est.	Err.	True	Est.	Err.	True	Est.	Err.
0.0547	0.0520	350	349	-0.4	350	325	-7.3	350	336	-3.9	4.1	3.9	-3.9
		480	480	-0.1	480	446	-7.0	480	463	-3.6	2.1	2.0	-5.6
		580	581	1.9	570	483	-15.2	570	530	-7.1	6.1	5.6	-8.2

 Table 10: Results for case A obtained by the NM method considering only data for  $t < 100$  h

early-time radial flow is observed. For the second trial, pressure and flow-rate data for  $t < 1 \times 10^{-2}$  h were discarded. Thus, only late-time radial flow may be identified.

The results considering only data for  $t < 100$  h may be seen in Table 10. Again, the method was performed five times, yielding a difference lower than 1% between the results from each run, and Table 10 displays the results for the first run. One should recall that some data points were discarded and, therefore, the objective function value computed using the true set of parameters is slightly different than observed in Table 4.

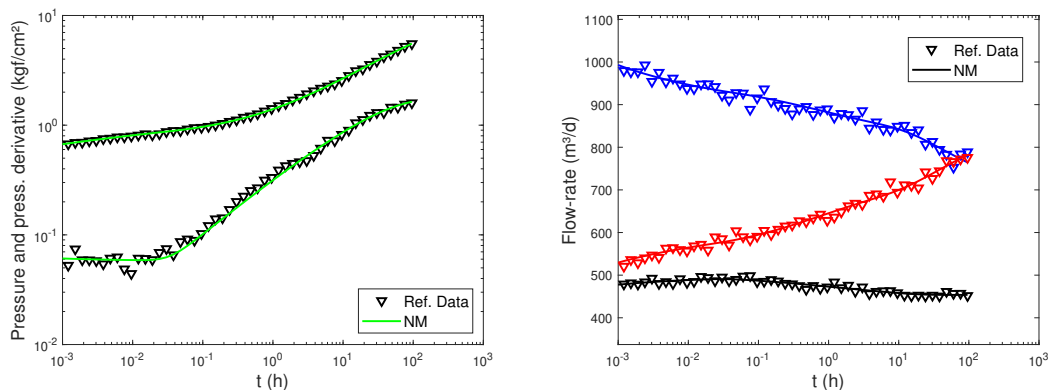
Layer properties were estimated with decent accuracy. This shows that the NM method was able to provide good estimates for layer horizontal permeabilities despite the fact that late-time radial flow was not identified before 100 hours. Figure 6 compares the reference data to the pressure and flow-rate profiles computed using layer properties exhibited in Table 10. A great match is observed. Results from Table 10 and Fig. 6 evidence that layer properties could be accurately determined using the NM algorithm, despite the fact that late-time radial flow data were discarded.

On the other hand, results were substantially worse when early-time data was discarded. Table 11 exhibits the estimated layer properties at each individual method run. As evidenced in Table 11, the method only converged in three out of the five runs, although the objective function at the last iteration presented similar values. Moreover, permeabilities in the  $z$ -direction and layer mechanical skins showed significant differences at each run. These results suggest that early-time data are critical to accurately determine  $k_{zj}$  and  $S_j$  in each layer.

Despite that, it is interesting to observe that layer horizontal permeabilities were determined with good precision in all runs. This is a relevant outcome, as it shows that the NM method may provide good estimates for  $k_{xyj}$  even if early-time data is not available.

## 5 Summary and Conclusions

This work provides methods for determining layer permeabilities and skin in multilayer reservoirs with multilateral wells. We extended the RNPA (rate normalized pressure analysis) (Ehlig-


 Fig. 6: Comparison between estimated and reference pressure (left) and flow-rate data (right) considering only data for  $t < 100$  h

Parameter	True	1st run	2nd run	3rd run	4th run	5th run
Convergence	N/A	Conv.	Not	Conv.	Conv.	Not
$O(x)$	0.0513	0.04937	0.04969	0.04963	0.04940	0.04970
$k_{xyj}$	350	351	349	349	351	350
	480	485	485	485	485	484
	570	582	576	575	584	578
$k_{zxxj}$	350	391	260	260	434	325
	480	569	509	511	602	449
	570	613	639	565	659	515
$S_j$	4.1	3.5	7.1	7.1	2.8	4.7
	2.1	1.4	1.4	1.3	1.1	2.8
	6.1	6.6	4.5	6.0	6.1	7.8

Table 11: Estimated layer properties obtained by the NM method at each run considering only data for  $t > 1 \times 10^{-2}$  h

Economides and Joseph, 1987; Raghavan, 1989) and the DTM (delta transient method) (Galvão and Guimarães, 2017; Guimarães and Galvão, 2017) for multilayer reservoirs with multilateral horizontal wells. These methods demand only a simple spreadsheet software to be performed. The proposed applications of RNPA and DTM in reservoirs with multilateral horizontal wells rely on a clear identification of early- and late-time radial flow regimes.

In a practical case, however, early radial flow may not occur due to wellbore storage effects and small reservoir thickness (Goode and Thambynayagam, 1987; Odeh and Babu, 1990). Besides, the test may also end before the start of late-time radial flow, which is also delayed if the wellbore lateral lengths are too long (Ozkan et al., 1989; Kuchuk et al., 1991). Thereby, the Nelder-Mead optimization algorithm (NM) (Nelder and Mead, 1965) was also applied to estimate layer permeabilities and skin factors. The NM method does not rely on the identification of any particular flow regime. It requires, though, a computational implementation of the analytical model for pressure change developed by Pan et al. (2010) and several layer flow-rate measurements throughout the test. The objective function to be minimized accounts for both wellbore pressure and layer flow-rate profiles.

The proposed techniques were applied on a pair of synthetic cases. To represent a more realistic condition, artificial noise was added to the pressure and flow-rate data. Results showed that all methods yielded good estimates for layer permeability and successfully identified anisotropy effects. However, only the NM algorithm yielded decent estimates for layer mechanical skins, while both the RNPA and DTM failed to provide good estimates for the individual layer mechanical skin factors. Late-time radial flow data provided decent estimates for layer total skins using the RNPA and DTM. Nonetheless, the errors are highly magnified when these total skin estimates are used to compute the mechanical skin factors.

The parameters computed from RNPA and DTM presented errors with similar magnitude. It is important to highlight, though, that DTM requires the production logging data at only four distinct time steps (two at early-time and two at late-time), while the RNPA demands several flow-rate measurements. In this work, 6 distinct flow-rate measurements per radial flow regime (resulting in 12 distinct flow-rate points) were used to perform the RNPA. Thus, considering the operational advantage of DTM, this method is preferable to RNPA for a real field application.

Using the NM algorithm, it was possible to obtain good estimates and also avoid generating sets of layer properties that presented significant errors despite yielding a pressure response similar to the reference data. Nonetheless, application of the NM method requires the layer flow-rate profiles to be known. Since this work used the synthetic data obtained from an analytical model, determining layer flow-rates at each time step was not an issue. This, however, may be an operational setback for the successful application of the NM algorithm in a real field case.

Applications of the NM method were also made considering that either early- or late-time radial flow regime are not identified during the test. Results show that this technique is able to provide good estimates for layer horizontal permeabilities even under those circumstances. However, layer

permeabilities in the  $z$ -direction and mechanical skin factors could not be accurately determined by the NM method when early-time data were discarded.

In summary, both RNPA and DTM provided a simple way to accurately evaluate layer permeabilities but were not able to accurately estimate layer skin factors. Since DTM presents a relevant operational advantage, we recommend its use for real field applications, instead of RNPA. However, if a detailed layer flow-rate profile is available and the radial flow regimes are not clearly observed, then the NM algorithm can be used. This method yielded the best estimates for layer properties between the three tested techniques, despite being more computationally expensive.

## Nomenclature

$B$  = Formation volume factor ( $\text{m}^3/\text{m}^3$  std or B/STB)  
 $c$  = Compressibility ( $(\text{Pa})^{-1}$  or  $(\text{kgf}/\text{cm}^2)^{-1}$  or  $(\text{psi})^{-1}$ )  
 $dz$  = Smallest distance between the a wellbore lateral and a vertical boundary (m or ft)  
 $e$  = Exponent required to compute the geometric pseudo-skin in Eq. (11)  
 $h$  = Thickness (m or ft)  
 $k$  = Permeability ( $\text{m}^2$  or mD)  
 $L$  = Length of the wellbore lateral (m or ft)  
 $m$  = Constant derivative level attained during early or late radial flow  
 $n$  = Number of reservoir layers  
 $N_{me}$  = Number of distinct time steps when pressure and flow-rate have been measured  
 $O$  = Objective function to be minimized by the Nelder-Mead algorithm  
 $p$  = Pressure (Pa or  $\text{kgf}/\text{cm}^2$  or psi)  
 $p_N$  = Rate-normalized pressure change  
 $q$  = Flow-rate ( $\text{m}^3/\text{s}$  or STB/d or  $\text{m}^2/\text{d}$ )  
 $r$  = Radius (m or in or ft)  
 $S$  = Skin factor  
 $S_g$  = Pseudo-skin that occurs due to stream lines convergence, defined in Eq. (11)  
 $t$  = Time (s or h or d)  
 $x$  = Vector of model parameters in the Nelder-Mead algorithm  
 $\alpha$  = Coefficients required to perform the Nelder-Mead algorithm  
 $\beta$  = Beta transient parameter, defined in Eq. (22)  
 $\delta$  = Delta transient parameter, defined in Eq. (22)  
 $\gamma$  = Euler constant, equal to 0.57722  
 $\mu$  = Viscosity (cP or Pa·s)  
 $\phi$  = Porosity  
 $\sigma$  = Instant sources integral, defined in Eq. (A-2)  
 $\tau$  = Silent time integration variable

## Subscripts

$c$  = Contraction  
 $e$  = Expansion  
 $eq$  = Equivalent  
 $erf$  = Related to the early-time radial flow regime  
 $i$  = Simplex element index  
 $j$  = Layer index  
 $k$  = Time step index  
 $lrf$  = Related to the late-time radial flow regime  
 $r$  = Reflection  
 $s$  = Shrinkage

$t$  = Total  
 $wf$  = Well face  
 $x$  = Related to  $x$  direction  
 $xy$  = Related to  $xy$ -plane  
 $y$  = Related to  $y$  direction  
 $z$  = Related to  $z$  direction  
 $zx$  = Related to  $zx$ -plane

## Acknowledgements

Authors are grateful to Petrobras for partially sponsoring this research as part of the project TCBR 485. This study was financed in part by the Coordenação de Aperfeiçoamento de Pessoal de Nível Superior - Brasil (CAPES) - Finance Code 001. The first author also thanks M.Sc. Thiago Silva for his helpful comments that improved this manuscript. Some parts of this study were completed while the first author was a visiting scholar at the University of Tulsa from February 2nd, 2020 until May 28th, 2020.

## Data Availability

This work is theoretical and does not contain any real field data.

## Ethics Declarations

### Conflict of Interest

Authors declare that they do not have any conflict of interest.

## References

- Algharaib, M., Gharbi, R., and Malallah, A. (2006). Scaling immiscible displacement in porous media with horizontal wells. *Transport in Porous Media*, 65:89–105.
- Aly, A., Chen, H. Y., and Lee, W. J. (1994). A new technique for analysis of wellbore pressure from multi-layered reservoirs with unequal initial pressures to determine individual layer properties. *Eastern Regional Conference and Exhibition*, November:1–15.
- Barati, R. (2011). Parameter estimation of nonlinear muskingum models using nelder-mead simplex algorithm. *Journal of Hydrologic Engineering*, November:946–954.
- Biryukov, D. and Kuchuk, F. J. (2015). Pressure transient behavior of horizontal wells intersecting multiple hydraulic fractures in naturally fractured reservoirs. *Transport in Porous Media*, 110:369–408.
- Boughara, A. A. and Reynolds, A. C. (2009). Analysis of injection/falloff data from horizontal wells. *SPE Journal*, December:721–736.
- Clonts, M. D. and Ramey Jr., H. J. (1986). Pressure-transient analysis for wells with horizontal drainholes. *paper presented at SPE California Regional Meeting*, April:215–230.
- Cobb, W. M., Jr., H. J. R., and Miller, F. G. (1972). Well-test analysis for wells producing commingled zones. *Journal of Petroleum Technology*, January:27–37.
- Daviau, F., Mouronvai, G., Bourdarot, G., and Curutchet, P. (1988). Pressure analysis for horizontal wells. *SPE Formation Evaluation*, December:716–724.
- Ehlig-Economides, C. A. and Joseph, J. (1987). A new test for determination of individual layer properties in a multilayered reservoir. *SPE Evaluation Formation*, September:261–283.

- Feng, Z.-K., Niu, W.-J., Zhou, J.-Z., and Cheng, C.-T. (2020). Linking nelder-mead simplex direct search method into two-stage progressive optimality algorithm for optimal operation of cascade hydropower reservoirs. *Journal of Water Resources Planning and Management*, 146(5):04020019.
- Galvão, M. S. C. and Guimarães, C. S. (2017). A new method for calculating individual layer permeability and skin in a multilayered reservoir using production logging data: The delta transient method. *Paper presented at the SPE Latin America and Caribbean Mature Fields Symposium*, pages 1–30.
- Gao, C.-T. (1987). Determination of parameters for individual layers in multilayer reservoirs by transient well tests. *SPE Formation Evaluation*, March:43–65.
- Ghiasi, M. H., Pasini, D., and Lessard, L. (2007). Improved globalized nelder-mead method for optimization of a composite bracket. *International Conference on Composite Materials*, pages 1–9.
- Goode, P. A. and Thambynayagam, R. K. M. (1987). Pressure drawdown and buildup analysis of horizontal wells in anisotropic media. *SPE Formation Evaluation*, December:683–697.
- Guimarães, C. S. and Galvão, M. S. C. (2017). Application of the delta transient method to multi-rate tests: A method for calculating individual layer permeability and skin in a multilayered reservoir using production logging data. *Paper presented at the Offshore Technology Conference Brasil*, pages 1–22.
- Hawkins, M. F. (1956). A note on the skin effect. *Journal of Petroleum Technology*, December:65–66.
- Jelmert, T. A. and Thompson, L. G. (1991). Horizontal wells - a test on infinite conductivity solutions. *Paper presented at SPE International Arctic Technology Conference*, May:1–20.
- Joshi, S. D. (2003). Costs/benefits of horizontal wells. *paper presented at SPE Western Regional/AAPG Pacific Section Joint Meeting*, May:1–9.
- Kuchuk, F. (1995). Well testing and interpretation for horizontal wells. *Journal of Petroleum Technology*, January:36–41.
- Kuchuk, F., Karakas, M., and Ayestaran, L. (1986a). Well testing and analysis techniques for layered reservoirs. *SPE Formation Evaluation*, August:342–354.
- Kuchuk, F. J., Goode, P. A., Wilksinson, D. J., and Thambynayagam, R. K. M. (1991). Pressure-transient behavior for horizontal wells with and without gas cap or aquifer. *SPE Formation Evaluation*, March:86–94.
- Kuchuk, F. J., Shah, P. C., Ayestaran, L., and Nicholson, B. (1986b). Application of multilayer testinf and analysis: a field case. *Paper presented at the SPE Annnual Technical Conference and Exhibition*, October:1–16.
- Kuchuk, F. J. and Wilkinson, D. J. (1991). Transient pressure behavior of commingled reservoirs. *SPE Formation Evaluation*, March:111–120.
- Larsen, L. (1981). Wells producing commingled zones with unequal initial pressures and reservoir properties. *Annual Fall Technical Conference and Exhibition of SPE*, October:1–29.
- Larsen, L. (1982). Determination of skin factors and flow capacities of individual layers in two-layered reservoirs. *Annual Fall Technical Conference and Exhibition of SPE*, September:1–16.
- Larsen, L. (2000). Pressure-transient behavior of multibranching wells in layered reservoirs. *SPE Reservoir Evaluation & Engineering*, February:68–73.
- Lefkovits, H. C., Hazebroek, P., Allen, E. E., and Matthews, C. S. (1961). A study of the behavior of bounded reservoirs composed of stratified layers. *SPE Journal*, March:43–58.
- Luersen, M. A. and Le Riche, R. (2004). Globalized nelder-mead method for engineering optimization. *Computers & Structures*, 82:23–26.
- Nelder, J. A. and Mead, R. (1965). A simplex method for function optimization. *Computers & Structures*, 7:308–313.
- Nie, R.-S., Meng, Y.-F., Jia, Y.-L., Zhang, F.-X., Yang, X.-T., and Niu, X.-N. (2011). Dual porosity and dual permeability modeling of horizontal well in naturally fractured reservoir. *Transport in Porous Media*, 92:213–235.
- Odeh, A. S. and Babu, D. K. (1990). Transient flow behavior of horizontal wells, pressure drawdown and buildup analysis. *SPE Formation Evaluation*, March:7–15.
- Ozkan, E., Raghavan, R., and Joshi, S. D. (1989). Horizontal well pressure analysis. *SPE Formation Evaluation*, December:567–575.

- Pan, Y., Kamal, M. M., and Kikani, J. (2010). Field applications of a semianalytical model of multilateral wells in multilayer reservoirs. *SPE Reservoir Evaluation & Engineering*, December:861–872.
- Raghavan, R. (1989). Behavior of wells completed in multiple producing zones. *SPE Evaluation Formation*, June:219–230.
- Raghavan, R., Topaloglu, H. N., Cobb, W. M., and Jr., H. J. R. (1974). Well-test analysis for wells producing from two commingled zones of unequal thickness. *Journal of Petroleum Technology*, September:1035–1043.
- Rahmati, H., Nouri, A., Pishvaie, M. R., and Bozorghmery, R. (2013). A modified differential evolution optimization algorithm with random localization for generation of best-guess properties in history matching. *Energy Sources, Part A: Recovery, Utilization and Environmental Effects*, June:845–858.
- Rosa, A. J. and Carvalho, R. d. S. (1989). A mathematical model for pressure evaluation in an infinite-conductivity horizontal well. *SPE Formation Evaluation*, December:559–566.
- Vo, D. T. and Madden, M. V. (1995). Performance evaluation of trilaterals: Field examples. *SPE Reservoir Engineering*, February:22–28.
- Yildiz, T. (2003). Multilateral pressure-transient response. *SPE Journal*, March:5–12.

## A Mathematical Model

The considered mathematical model assumes the single-phase isothermal flow of a slightly compressible fluid with constant viscosity and compressibility. Gravitational and wellbore storage effects are neglected.

It is assumed a multilayer stratified reservoir with a multilateral horizontal well, such that each layer is perforated by exactly one well ramification. Since no formation crossflow is assumed, a multilateral well is required so that the influence of all layers is felt in pressure response. Moreover, it is considered that each wellbore branch is parallel to the horizontal plane. It was also assumed that the effective wellbore length of each branch is known. In practice, the total drilled length does not necessarily match the well effective length, which might be challenging to determine (Boughara and Reynolds, 2009; Pan et al., 2010).

By model hypothesis, pressure is the same in all layers, apart from the hydrostatic column. It is considered a transversely isotropic system, that is, permeability along the horizontal plane ( $k_{xyj}$ ) is constant but the vertical permeability ( $k_{zj}$ ) might be different. All computations assume that a consistent set of units is used.

### A.1 Pressure solution for single-layer reservoirs

The real space solution for single-layer reservoirs with horizontal wells was developed by Daviau et al. (1988) and Ozkan et al. (1989). They considered that the wellbore may be depicted as a line sink. Then, using Newman's product and Green's functions, pressure change is decomposed as the product of three terms, each one related to the transient pressure pulse propagation in a given direction (Rosa and Carvalho, 1989):

$$\Delta p(x, y, z, t) = \frac{q}{L\phi c_t} \sigma(x, y, z, t) + \frac{q\mu}{k_{zx}L} S \quad (\text{A-1})$$

where  $k_{zx} = \sqrt{k_{xy}k_z}$  is the geometric permeability in the  $zx$ -plane and  $\sigma(x, y, z, t)$  is defined as:

$$\sigma(x, y, z, t) = \int_0^t \frac{\exp\left(-\frac{(x-x_1)^2}{4\eta_{xy}\tau}\right)}{2\sqrt{\pi\eta_{xy}\tau}} \frac{1}{2} \left[ \operatorname{erf}\left(\frac{y_1 + L - y}{2\sqrt{\eta_{xy}\tau}}\right) - \operatorname{erf}\left(\frac{y_1 - y}{2\sqrt{\eta_{xy}\tau}}\right) \right] \cdot \frac{1}{2\sqrt{\pi\eta_z\tau}} \left[ \sum_{n=-\infty}^{\infty} \exp\left(-\frac{(2nh)^2}{4\eta_z\tau}\right) + \exp\left(-\frac{(2nh - 2dz)^2}{4\eta_z\tau}\right) \right] d\tau \quad (\text{A-2})$$

In Eqs. (A-1) and (A-2),  $S$  stands for the mechanical skin factor as proposed by Hawkins (1956), the hydraulic diffusivity in the horizontal plane is defined as  $\eta_{xy} = k_{xy}/\phi\mu c_t$ , where  $\phi$  is the reservoir porosity,  $\mu$  denotes the fluid viscosity and  $c_t$  represents the total compressibility. The diffusivity in  $z$ -direction ( $\eta_z$ ) is analogously defined. Wellbore length is denoted by  $L$ , while  $h$  stands for the reservoir thickness and  $dz$  represents the smallest distance between the wellbore and a vertical boundary. The point with coordinates  $(x_1, y_1, z_1)$  represents the wellbore heel.

The integral term defined in Eq. (A-2) represents the instantaneous pressure change due to the oil production of all sink points along the well path, considering a constant flow-rate  $q$ . Therefore, Eq. (A-1) shows that pressure change at the wellbore is given by the time integral of all instant pressure changes caused by the sink well.

Eq. (A-1) was achieved under the assumption of uniform flux along the wellbore (Daviau et al., 1988; Ozkan et al., 1989). Nonetheless, this hypothesis does not match the physical reality of flow in horizontal wells, since it implies that pressure at the well midpoint is lower than at the well tips. Considering that pressure (instead of fluid inflow) is uniform along the well is a more realistic approach (Rosa and Carvalho, 1989; Jelmert and Thompson, 1991). Pressure behavior in an infinite conductivity well may be determined from Eq. (A-1) using either the equivalent pressure point (Ozkan et al., 1989) or the average pressure method (Goode and Thambynayagam, 1987; Kuchuk et al., 1991).

## A.2 Pressure solution for multilayer reservoirs

The real space solution for multilayer reservoirs was achieved by Pan et al. (2010). They assumed that layer flow-rate profile is depicted by a step-wise constant function. Then, Eq. (A-1) may be combined with the superposition principle to obtain an expression for the pressure change in each layer at the  $k$ -th timestep:

$$\Delta p_j(x, y, z, t_k) = \sum_{m=1}^k \left( \frac{q_j^m - q_j^{m-1}}{L_j \phi_j c_{tj}} \right) \sigma_j(x, y, z, t), \quad \text{for } j = 1, \dots, n \quad (\text{A-3})$$

where  $n$  is the total number of layers and  $\sigma_j(x, y, z, t)$  denotes the integral term defined in Eq. (A-2), evaluated using the properties of layer  $j$ .

Eq. (A-3) is derived from the single-lateral solution developed by Daviau et al. (1988) and Ozkan et al. (1989). Thus, it assumes uniform flux at each wellbore branch. Considering an infinite conductivity well, pressure change at each time step must be the same in all layers. Furthermore, mass balance at the well assure that the sum of all layer flow-rates must be equal to the total production flow-rate. Thus, the following linear system may be written for a  $n$ -layer reservoir at each time step (Pan et al., 2010):

$$\begin{cases} \sum_{j=1}^n q_j^k = q_t \\ \Delta p_j(t_k) = \Delta p_{j+1}(t_k), \end{cases} \quad \text{for } j = 1, \dots, n-1 \quad (\text{A-4})$$

At each time step, after the linear system defined in Eq. (A-4) is solved, pressure change may be computed by applying Eq. (A-3) at any layer. To obtain a more accurate response, each well lateral may be discretized into several well segments, which increases the order of the linear system defined in Eq. (A-4).

The solution developed by Pan et al. (2010) is, in fact, more general and also applies for multi-lateral wells in single-layer reservoirs, or multilayer systems with more than one well branch in each layer. However, these applications are not detailed here, since the goal of this work is to compute individual layer properties assuming the wellbore-reservoir schematics portrayed in figure 1. Although the analytical models for single (Daviau et al., 1988; Ozkan et al., 1989) and multilayer reservoirs (Pan et al., 2010) account for horizontal anisotropy, permeability in the  $x$ - and  $y$ -directions were assumed to be equal in this work.

## B Nelder-Mead Algorithm

The Nelder-Mead algorithm (NM) is a gradient free optimization method that aims to minimize a  $n$ -variables function  $O(x)$ , where  $x = \{x_1, x_2, \dots, x_n\}$  is a vector containing the  $n$  variables of the problem (Nelder and Mead, 1965).

NM starts by setting a simplex composed of  $n + 1$  vertices. Then, the function is evaluated at each simplex vertex. Then, the vertices associated with the maximum and minimum function values are defined as  $x_H$  and  $x_L$ , respectively. The goal at each iteration is to replace  $x_H$  until a convergence criteria is reached (Rahmati et al., 2013; Feng et al., 2020).

Depending on the objective function values, four distinct operations may be performed to update the simplex: reflection, expansion, contraction and shrinkage. An operation is considered successful if it yields a new minimum. The reflection operation is defined as (Nelder and Mead, 1965; Luersen and Le Riche, 2004):

$$x_r = (1 + \alpha_r)\bar{x} - \alpha_r x_L, \quad (\text{B-1})$$

where  $\bar{x}$  represents the centroid of all simplex points excluding  $x_H$  and  $\alpha_r$  is a positive constant denoted as reflection coefficient.

Reflection is considered successful if  $O(x_r) < O(x_L)$ , that is, if the reflected vertex represents a new minimum. If reflection succeeds, expansion is performed. This operation is defined as (Nelder and Mead, 1965; Ghiasi et al., 2007):

$$x_e = \alpha_e x_r + (1 - \alpha_e)\bar{x}, \quad (\text{B-2})$$

where  $\alpha_e$  is the expansion coefficient, which must be higher than 1. If expansion succeeds, then  $x_H$  is replaced by  $x_e$ . Otherwise, if reflection succeeds but expansion fails,  $x_H$  is replaced by  $x_r$ .

If reflection fails, then it must be determined whether the reflected vertex is a new maximum, that is, if  $O(x_r) > O(x_i)$ ,  $\forall x_i \neq x_H$ . If the reflected vertex is not a new maximum, then  $x_H$  is replaced by  $x_r$ . Otherwise, contraction is performed. The contracted vertex is computed as (Nelder and Mead, 1965; Feng et al., 2020):

$$x_c = \alpha_c x_{aux} + (1 - \alpha_c)\bar{x}, \quad (\text{B-3})$$

where:

$$x_{aux} = \begin{cases} x_H & \text{if } O(x_H) > O(x_r) \\ x_r & \text{otherwise} \end{cases} \quad (\text{B-4})$$

and  $\alpha_c$  is the contraction coefficient, which lies inside the interval  $[0, 1]$ .

If contraction succeeds, then  $x_H$  is replaced by  $x_c$ . Otherwise, shrinkage is performed. This operation consists of multiplying all simplex vertices, except for  $x_L$  by a coefficient between zero and one, the shrinkage coefficient  $\alpha_s$  (Nelder and Mead, 1965; Barati, 2011):

$$x_i = \alpha_s x_i \quad \forall x_i \neq x_L. \quad (\text{B-5})$$

After the simplex has been updated, the suitable convergence criteria is tested. This process is repeated until convergence is reached. In this work, the parameters  $\alpha_r$ ,  $\alpha_e$ ,  $\alpha_c$  and  $\alpha_s$ , required to perform the simplex operations, were set as 1.0, 2.0, 0.5 and 0.5, respectively. Nelder and Mead

(1965) and Barati (2011) applied these values and showed that they provide good convergence. The Nelder-Mead optimization algorithm was originally proposed for unconstrained domains (Nelder and Mead, 1965). However, linear constraints may be easily coupled to the algorithm (Ghiasi et al., 2007). Considering that, for each variable, a range that must contain the minimum has been specified, the boundary constraints are coupled to the algorithm by checking, after each operation, if the new simplex vertex is within the specified range. If the updated simplex vertex falls out of the bounded range, then it is projected to the bounded region defined by the maximum and minimum acceptable values (Luersen and Le Riche, 2004). Thus, if a given simplex coordinate  $x_i$  is out of the specified range, the projection is made as follows:

$$x_i := \begin{cases} x_i^{max} & \text{if } x_i > x_i^{max} \\ x_i^{min} & \text{if } x_i < x_i^{min} \end{cases} \quad (\text{B-6})$$

In summary, the algorithm workflow goes as follows:

- Step 1 Define the initial simplex (for instance, by randomly choosing the vertices).
- Step 2 Evaluate the objective function at each simplex vertex and identify  $x_H$  and  $x_L$ .
- Step 3 Perform the reflection operation as defined in Eq. (B-1). If reflection succeeds, proceed to step 4. Otherwise, proceed to step 5.
- Step 4 Perform the expansion operation, as defined in Eq. (B-2). If expansion succeeds, update the simplex by replacing  $x_H$  by  $x_e$ . Otherwise, update the simplex by replacing  $x_H$  by  $x_r$ . Next, proceed to step 8.
- Step 5 If reflection yielded a new maximum, proceed to step 6. Otherwise, update the simplex by replacing  $x_H$  by  $x_e$  and proceed to step 8.
- Step 6 Perform the contraction operation, as defined in Eq. (B-3). If contraction succeeds, update the simplex by replacing  $x_H$  by  $x_c$  and proceed to step 8. Otherwise, proceed to step 7.
- Step 7 Update the simplex by performing the shrinkage operation, as defined in Eq. (B-5). Next, proceed to step 8.
- Step 8 Apply the convergence criteria to the updated simplex. If convergence is not reached, iterate again by going back to step 2.